

# Thermoelectric power generator module of $16 \times 16$ $\text{Bi}_2\text{Te}_3$ and 0.6% ErAs: $(\text{InGaAs})_{1-x}(\text{InAlAs})_x$ segmented elements

Gehong Zeng,<sup>1,a)</sup> Je-Hyeong Bahk,<sup>1</sup> John E. Bowers,<sup>1</sup> Hong Lu,<sup>2</sup> Arthur C. Gossard,<sup>2</sup> Suzanne L. Singer,<sup>3</sup> Arun Majumdar,<sup>3</sup> Zhixi Bian,<sup>4</sup> Mona Zebarjadi,<sup>4</sup> and Ali Shakouri<sup>4</sup>

<sup>1</sup>Department of Electrical and Computer Engineering, University of California, Santa Barbara, California 93106, USA

<sup>2</sup>Department of Materials, University of California, Santa Barbara, California 93106, USA

<sup>3</sup>Department of Mechanical Engineering, University of California, Berkeley, California 94720, USA

<sup>4</sup>Department of Electrical Engineering, University of California, Santa Cruz, California 95064, USA

(Received 22 April 2009; accepted 3 August 2009; published online 26 August 2009)

We report the fabrication and characterization of thermoelectric power generator modules of  $16 \times 16$  segmented elements consisting of 0.8 mm thick  $\text{Bi}_2\text{Te}_3$  and 50  $\mu\text{m}$  thick ErAs:  $(\text{InGaAs})_{1-x}(\text{InAlAs})_x$  with 0.6% ErAs by volume. An output power up to 6.3 W was measured when the heat source temperature was at 610 K. The thermoelectric properties of  $(\text{InGaAs})_{1-x}(\text{InAlAs})_x$  were characterized from 300 up to 830 K. The finite element modeling shows that the performance of the generator modules can further be enhanced by improving the thermoelectric properties of the element materials, and reducing the electrical and thermal parasitic losses. © 2009 American Institute of Physics. [DOI: 10.1063/1.3213347]

Solid state thermoelectric generator modules composed of  $n$  and  $p$  semiconductor element couples can be used for direct thermal to electrical energy conversion. Their great potential in providing cleaner form of energy and reducing environmental contamination has been recognized. The power conversion performance of a thermoelectric generator module depends largely on the semiconductor element's thermoelectric properties, in terms of the thermoelectric figure-of-merit,  $Z = \alpha^2 \cdot \sigma / \kappa$ , where  $\alpha$  is the Seebeck coefficient,  $\sigma$  is the electrical conductivity, and  $\kappa$  is the thermal conductivity. The quantum confinement effects of these low dimensional structures can improve the material's power factor ( $\alpha^2 \sigma$ ).<sup>1,2</sup> Lattice thermal conductivity can be reduced due to the increase of phonon scattering by abundant surfaces and interfaces in nanostructured materials.<sup>3,4</sup> And the Seebeck coefficient can be increased through energy filtering by thermionic emission across heterointerfaces,<sup>5,6</sup> and/or energy-dependent electron scattering by nanostructures.<sup>7,8</sup> Thermal conductivity reduction using superlattice heterostructures or incorporation of nanoparticles has been demonstrated.<sup>9–11</sup> In this study, ErAs nanoparticles were epitaxially incorporated into  $(\text{InGaAs})_{1-x}(\text{InAlAs})_x$  using molecular beam epitaxy (MBE). When ErAs nanoparticles are incorporated into  $(\text{InGaAs})_{1-x}(\text{InAlAs})_x$ , a bending potential barrier is formed at the interface between the particle and semiconductor. The Seebeck coefficient can be enhanced through the electron filtering effects of these potential barriers.<sup>12</sup> The performance of a thermoelectric generator module can be effectively enhanced by using segmented element structures with materials whose thermoelectric properties are optimized in successive temperature ranges.<sup>13</sup>

In this paper, we report the fabrication, characterization, and measurement of generator modules using segmented elements of 50  $\mu\text{m}$  0.6% ErAs:  $(\text{InGaAs})_{1-x}(\text{InAlAs})_x$  and 0.8 mm  $\text{Bi}_2\text{Te}_3$  (Fig. 1).

$(\text{InGaAs})_{0.8}(\text{InAlAs})_{0.2}$  samples with 0%, 0.3%, and 0.6% ErAs volume concentrations were grown on lattice-matched InP(100) substrates of 520  $\mu\text{m}$  thick using MBE with the growth temperature maintained at 490 °C. The thermal conductivity of the 2  $\mu\text{m}$  epitaxial thin film layers were measured using  $3\omega$  method.<sup>14</sup> The measurement results (Fig. 2) show that by incorporating ErAs nanoparticles in InGaAlAs, the thermal conductivity was reduced below that of the alloy  $(\text{InGaAs})_{0.8}(\text{InAlAs})_{0.2}$ . By increasing the ErAs concentration from 0.3% to 3%, the thermal conductivity of the material is further reduced by about 25%.

To avoid any side effects from InP substrate in Seebeck coefficient and electrical conductivity measurements, the semi-insulating InP substrate was removed in our material characterization. The epitaxial sample was bonded onto a sapphire substrate using a  $\text{SiO}_2$ – $\text{SiO}_2$  oxide bonding technique.<sup>15</sup> Then, the semi-insulating InP was removed by wet etching leaving just the 2  $\mu\text{m}$  epitaxial layer of bonded onto a 500  $\mu\text{m}$  sapphire substrate. TiWN was used as metal diffusion barrier, which has good barrier property and thermal stability up to 700 °C.<sup>16</sup> Measurement results (Fig. 3) show that the Seebeck coefficient increases with temperatures from 300 to 830 K, and the electrical conductivity increases with temperatures from 300 to 600 K, but the values become saturated when the temperature is over 600 K. The reason is that the electron-phonon and electron-nanoparticle scatterings become stronger at high temperatures, and the

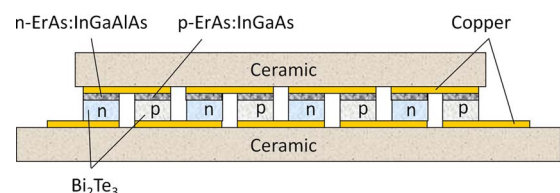


FIG. 1. (Color online) Schematic structure of the segmented element generator module of ErAs:InGaAlAs and  $\text{Bi}_2\text{Te}_3$ .

<sup>a)</sup>Electronic mail: gehong@ece.ucsb.edu.

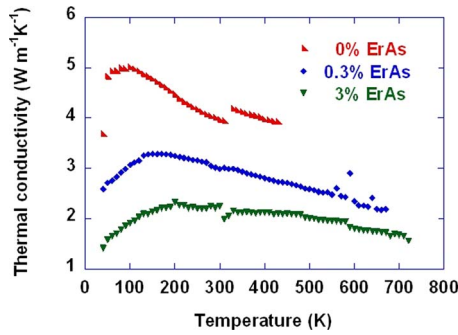


FIG. 2. (Color online)  $3\omega$  measurement results of thermal conductivity for  $(\text{InGaAs})_{0.8}(\text{InAlAs})_{0.2}$  with the ErAs concentration of 0%, 0.3%, and 3%, respectively.

carrier mobility is reduced significantly even though the carrier concentration still increases with temperature moderately. The comparison of  $ZT$  values between  $\text{Bi}_2\text{Te}_3$  and ErAs:InGaAlAs (Fig. 4) indicates that it can be beneficial by using segmented elements of the two materials.

The characterization of  $p$ -ErAs:InGaAs material was carried out using the same measurement method as that used for  $n$ -ErAs:InGaAlAs. Their thermoelectric properties are comparable up to 400 K. When the temperature increases from 400 to 600 K,  $n$ -ErAs:InGaAlAs shows larger power factor than that of  $p$ -ErAs:InGaAs.

Two  $50\ \mu\text{m}$  0.6% ErAs:  $(\text{InGaAs})_{1-x}(\text{InAlAs})_x$  for segmented generator modules were grown on lattice-matched InP(100) substrates using MBE with the same material structure as that of the  $2\ \mu\text{m}$  characterization samples. The  $n$ -type ErAs:  $(\text{InGaAs})_{1-x}(\text{InAlAs})_x$  consists of 80% InGaAs and 20% InAlAs, while the  $p$ -type sample is ErAs:InGaAs.

Ni/GeAu/Ni/Au contact metals were used for  $n$ -type ErAs:InGaAlAs, and Pt/Ti/Pt/Au were used for  $p$ -type ErAs:InGaAs, respectively. Then TiWN was deposited on the contact metal layers and used as a metal barrier layer to prevent metal diffusion at high temperatures. The transmission line measurements show that the contact resistance for both  $n$  and  $p$  types are less than  $8 \times 10^{-7}\ \Omega\ \text{cm}^2$ . The  $16 \times 16$  element array of  $\text{Bi}_2\text{Te}_3$  elements was bonded on a lower ceramic plate; while the  $16 \times 16$  ErAs:  $(\text{InGaAs})_{1-x}(\text{InAlAs})_x$  element array was bonded on an upper ceramic plate. And then the two ceramic plates were bonded together using flip-chip bonding technique to form a  $16 \times 16$  segmented element generator module.

An output power of 6.3 W was measured when the heat source temperature was at 610 K and the cooling water tem-

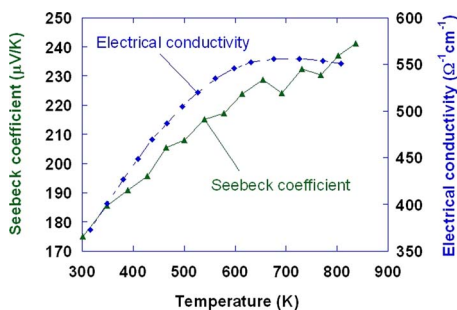


FIG. 3. (Color online) Variable temperature measurement results of the Seebeck coefficient and electrical conductivity of 0.6% ErAs  $(\text{InGaAs})_{0.8}(\text{InAlAs})_{0.2}$ .

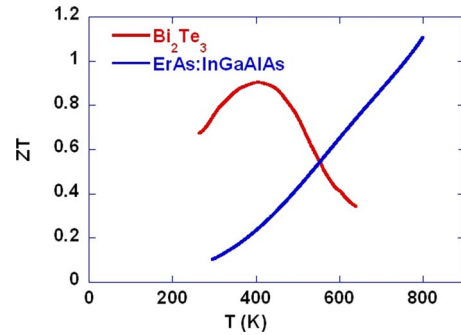


FIG. 4. (Color online) Comparison of  $ZT$  values for the  $\text{Bi}_2\text{Te}_3$  and ErAs:InGaAlAs from 300 up to 650 K.

perature was kept at 285 K. A three-dimensional (3D) finite element modeling was used for the analyses of the generator module performance, in which the Peltier, Seebeck, and Thomson effects were taken into account and the input parameters of material properties and contact resistances were from experimental data. The modeling results are compared with experimental measurements (Fig. 5). The thermal conductivity of the 0.7 mm thick ceramic plates used in the module is about  $26\ \text{W m}^{-1}\ \text{K}^{-1}$  (300 K), and the value decreases to  $12\ \text{W m}^{-1}\ \text{K}^{-1}$  at 600 K. Our modeling indicates that an improvement up to 6% can be expected by using 0.5 mm thick AlN plates with the thermal conductivity of  $175\ \text{W m}^{-1}\ \text{K}^{-1}$  at 300 K and around  $50\ \text{W m}^{-1}\ \text{K}^{-1}$  at 600 K. The specific contact resistance to  $\text{Bi}_2\text{Te}_3$  material is around  $6 \times 10^{-6}\ \Omega\ \text{cm}^2$ ; while the contact resistance to the ErAs:InGaAs is below  $8 \times 10^{-7}\ \Omega\ \text{cm}^2$ . 3D modeling shows that the performance of the generator module is improved by 4% by adding the  $50\ \mu\text{m}$  ErAs:InGaAlAs segment. Further improvement can be expected with the improvement of the element material properties, increasing the thickness of ErAs:  $(\text{InGaAs})_{1-x}(\text{InAlAs})_x$  elements, increasing heat source temperatures, and reducing the electrical and thermal parasitic losses.

In summary, MBE grown ErAs:  $(\text{InGaAs})_{1-x}(\text{InAlAs})_x$  samples with different ErAs concentrations were characterized by variable temperature measurements of thermal conductivity, electrical conductivity, and Seebeck coefficient from 300 up to 830 K. A  $16 \times 16$  thermoelectric power generator module was fabricated using segmented elements of  $50\ \mu\text{m}$  0.6% ErAs:  $(\text{InGaAs})_{1-x}(\text{InAlAs})_x$  and 0.8 mm

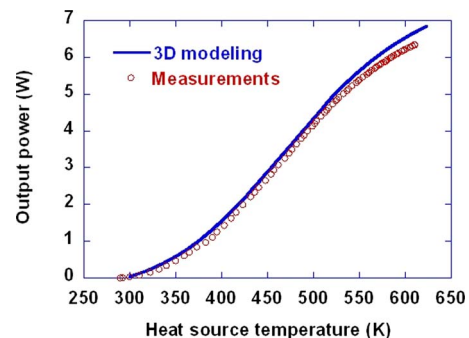


FIG. 5. (Color online) Comparison of the measurement results for the  $16 \times 16$  segmented element power generator module of  $50\ \mu\text{m}$  ErAs:  $(\text{InGaAs})_{1-x}(\text{InAlAs})_x$  and 0.8 mm  $\text{Bi}_2\text{Te}_3$  and 3D finite element modeling simulation.

$\text{Bi}_2\text{Te}_3$ . An output power of 6.3 W was measured with heat source temperature rising up to 610 K.

The authors acknowledge useful discussions with Dr. Mihai Gross. This work is supported by the Office of Naval Research through Contract No. N00014-05-1-0611. The generator module fabrication work was done in the UCSB nanofabrication facility, part of the NSF funded NNIN network.

<sup>1</sup>L. D. Hicks and M. S. Dresselhaus, *Phys. Rev. B* **47**, 16631 (1993).

<sup>2</sup>T. C. Harman, M. P. Walsh, B. E. Laforge, and G. W. Turner, *J. Electron. Mater.* **34**, L19 (2005).

<sup>3</sup>M. V. Simkin and G. D. Mahan, *Phys. Rev. Lett.* **84**, 927 (2000).

<sup>4</sup>C. Dames and G. Chen, *J. Appl. Phys.* **95**, 682 (2004).

<sup>5</sup>D. Vashaee and A. Shakouri, *J. Appl. Phys.* **95**, 1233 (2004).

<sup>6</sup>A. Shakouri and J. E. Bowers, *Appl. Phys. Lett.* **71**, 1234 (1997).

<sup>7</sup>T. C. Harman, P. J. Taylor, D. L. Spears, and M. P. Walsh, *J. Electron.*

*Mater.* **29**, L1 (2000).

<sup>8</sup>S. V. Faleev and F. Leonard, *Phys. Rev. B* **77**, 214304 (2008).

<sup>9</sup>R. Venkatasubramanian, E. Siivola, T. Colpitts, and B. O'Quinn, *Nature (London)* **413**, 597 (2001).

<sup>10</sup>W. Kim, S. L. Singer, A. Majumdar, D. Vashaee, Z. Bian, A. Shakouri, G. Zeng, J. E. Bowers, J. M. O. Zide, and A. C. Gossard, *Appl. Phys. Lett.* **88**, 242107 (2006).

<sup>11</sup>B. Poudel, Q. Hao, Y. Ma, Y. C. Lan, A. Minnich, B. Yu, X. Yan, D. Z. Wang, A. Muto, D. Vashaee, X. Y. Chen, J. M. Liu, M. S. Dresselhaus, G. Chen, and Z. Ren, *Science* **320**, 634 (2008).

<sup>12</sup>J. M. O. Zide, D. Vashaee, Z. X. Bian, G. Zeng, J. E. Bowers, A. Shakouri, and A. C. Gossard, *Phys. Rev. B* **74**, 205335 (2006).

<sup>13</sup>G. J. Snyder and T. S. Ursell, *Phys. Rev. Lett.* **91**, 148301 (2003).

<sup>14</sup>D. G. Cahill, *Rev. Sci. Instrum.* **61**, 802 (1990).

<sup>15</sup>D. Liang, A. W. Fang, H. Park, T. E. Reynolds, K. Warner, D. C. Oakley, and J. E. Bowers, *J. Electron. Mater.* **37**, 1552 (2008).

<sup>16</sup>S. Bhagat, H. Han, and T. L. Alford, *Thin Solid Films* **515**, 1998 (2006).